Zeolites

International Edition: DOI: 10.1002/anie.201601135
German Edition: DOI: 10.1002/ange.201601135

Open-Pore Two-Dimensional MFI Zeolite Nanosheets for the Fabrication of Hydrocarbon-Isomer-Selective Membranes on Porous Polymer Supports

Han Zhang[+], Qiang Xiao[+], Xianghai Guo, Najun Li, Prashant Kumar, Neel Rangnekar, Mi Young Jeon, Shaeel Al-Thabaiti, Katabathini Narasimharao, Sulaiman Nasir Basahel, Berna Topuz, Frank J. Onorato, Christopher W. Macosko, K. Andre Mkhoyan, and Michael Tsapatsis**

Abstract: *Two-dimensional zeolite nanosheets that do not contain any organic structure-directing agents were prepared from a multilamellar MFI (ML-MFI) zeolite. ML-MFI was first exfoliated by melt compounding and then detemplated by treatment with a mixture of H_2SO_4 and H_2O_2 (piranha solution). The obtained OSDA-free MFI nanosheets disperse well in water and can be used for coating applications. Deposits made on porous polybenzimidazole (PBI) supports by simple filtration of these suspensions exhibit an n-butane/isobutane selectivity of 5.4, with an n-butane permeance of 3.5×10^{-7} mol m^{-2} s^{-1} Pa^{-1} (ca. 1000 GPU).*

Suspensions of two-dimensional (2D) zeolite nanosheets can be used as building blocks for the fabrication of membranes and catalysts.[1–5] Multilamellar MFI (ML-MFI) zeolites with 1.5 unit cell MFI nanosheets assembled along their *b* axis have been reported by Ryoo and co-workers.[6,7] They were synthesized using an organic structure directing agent (OSDA) composed of long-chain alkyl groups and two quaternary ammonium head groups spaced by a C_6 alkyl linkage ($C_{22\text{-}6\text{-}6}$). The two ammonium moieties play a structure-directing role for the formation of the MFI crystal structure while the long-chain alkyl tails guide the formation of lamellar assemblies.[8,9] ML-MFI can be exfoliated to obtain single-layer 2D zeolite MFI nanosheets. Unlike other 2D materials (e.g., clays, graphene, MoS_2, BN, and WS_2),[10–14] for which exfoliation can be achieved by various solution-based methods, exfoliation of ML-MFI has only been reported by a polymer-melt-blending technique.[3,15] According to this method, polystyrene (PS) is mixed with ML-MFI, and then the mixture is melt-blended. During melt blending, the polymer chains penetrate into the ML-MFI and, in combination with the shear force generated by the rotating screws, cause exfoliation. Exfoliated 2D MFI nanosheets are obtained after PS removal, purification by density gradient centrifugation (DGC), and redispersion in organic solvents. The obtained MFI nanosheets are hydrophobic and can be dispersed in non-polar solvents such as toluene and octanol but not in water. Dispersion in water is desirable because it will enable layer-by-layer deposition for nanocomposite and thin-film fabrication.[16,17] Moreover, the exfoliated nanosheets contain the OSDA in their micropores, preventing their use as molecular sieves without further detemplation for OSDA removal. Recently, we have demonstrated that treatment with acid, according to a method reported earlier by Corma and co-workers, removes some of the OSDA and enables the dispersion of the nanosheets in ethanol.[4,18] There is still approximately 8 wt% of OSDA left after acid treatment, and the partially detemplated nanosheets cannot be dispersed in water[4] and do not exhibit microporosity by cryogenic Ar adsorption. Here, the main difference from this earlier work is the use of a concentrated sulfuric acid (H_2SO_4) and hydrogen peroxide (H_2O_2) mixture (piranha solution, H_2SO_4/H_2O_2 3:1, v/v) to treat as-synthesized or exfoliated ML-MFI particles. Furthermore, the method for the synthesis of pure silica ML-MFI was modified (see the Supporting Information) from previous reports,[3,6] and larger MFI nanosheet domains were obtained (Supporting Information, Fig-

[*] H. Zhang,[+] P. Kumar, N. Rangnekar, M. Y. Jeon, F. J. Onorato, Prof. C. W. Macosko, Prof. K. A. Mkhoyan, Prof. M. Tsapatsis
Department of Chemical Engineering and Materials Science
University of Minnesota
421 Washington Ave SE, Minneapolis, MN 55455 (USA)
E-mail: tsapatsis@umn.edu
Prof. Q. Xiao[+]
Key Laboratory of the Ministry of Education for Advanced Catalysis Materials, Institute of Physical Chemistry
Zhejiang Normal University, Jinhua, Zhejiang 321004 (China)
E-mail: xiaoq@zjnu.edu.cn
Prof. X. H. Guo
Key Laboratory of Systems Bioengineering, Ministry of Education
Department of Pharmaceutical Engineering
School of Chemical Engineering and Technology
Tianjin University, Tianjin 300072 (China)
Prof. N. J. Li
College of Chemistry, Chemical Engineering and Materials Science
Collaborative Innovation Center of Suzhou Nano Science and Technology
Soochow University, Suzhou, Jiangsu 215123 (China)
Prof. S. Al-Thabaiti, Prof. K. Narasimharao, Prof. S. N. Basahel
Department of Chemistry, Faculty of Science
King Abdulaziz University, Jeddah, 21589 (Saudi Arabia)
Prof. B. Topuz
Department of Chemical Engineering, Ankara University
Ankara 06100 (Turkey)
[+] These authors contributed equally to this work.
Supporting information and the ORCID identification number(s) for the author(s) of this article can be found under http://dx.doi.org/10.1002/anie.201601135.

ure S1 a) compared with those synthesized previously[3] (Figure S1 b).

First, we observed that sonication only did not significantly alter the multilamellar stacking. Treatment with mild acids followed by sonication showed similar outcomes. These failed attempts directed us to explore more aggressive approaches. Piranha solution is known as one of the strongest oxidizing agents used to remove organic residues. It was used here to decompose the OSDA in ML-MFI. The as-synthesized ML-MFI was treated with fresh piranha solution at 80 °C for one day. Thermogravimetric analysis (TGA) indicates that the weight loss (at 120–700 °C) decreased from approximately 35 % (as-synthesized ML-MFI) to 12.7 % after the first piranha solution treatment (Figure S2). The weight loss further decreased to 6.0 % when the above as-obtained product was treated with piranha solution for a second time under the same conditions and ultimately to 2.6 % after the fourth treatment (Figure S2). Argon adsorption measurements showed that the micropore volume had increased after the treatment had been repeated four times (Figure S3). An analogous sample that was calcined at 550 °C exhibited a similar micropore volume. These results suggest that most of the organic species were removed, and that the majority of the micropores were open after the repeated piranha solution treatment. Furthermore, the MFI crystallinity was preserved during all treatment stages, as confirmed by the MFI peaks in the wide-angle XRD pattern (Figure S4 A). ^{29}Si MAS NMR data indicate that the Q3/(Q3 + Q4) ratio in the piranha-solution-treated samples decreased in comparison to that of as-synthesized ML-MFI (0.17 vs. 0.21) and remained unaltered as the piranha treatment was repeated. At the same time, the low-angle XRD peaks that correspond to the layered structure had completely disappeared after the treatment had been repeated four times, indicating the loss of the multilamellar stacking. An ML-MFI sample that had been treated with the piranha solution six times did not show any changes in the XRD pattern (Figure S4 A) and the ^{29}Si MAS NMR spectrum (Figure S4 B). After treating ML-MFI with piranha solution, single-layer exfoliated nanosheets (Figure S5 a) mixed with larger aggregates (Figure S5 b) were obtained. The exfoliated nanosheets had lateral dimensions of up to 1 μm. 1.5 Unit cell MFI nanosheets with in-plane sizes larger than 1 μm have not been reported before (earlier reports indicate basal dimensions of up to 200 nm).[15] Conventional transmission electron microscopy (CTEM) shows the co-existence of non-exfoliated ML-MFI with individual layers stacked together (Figure 1 a) and exfoliated nanosheets (Figure 1 b). For the non-exfoliated portion, the MFI layers are arranged with a rotational misorientation about the [010] direction, visible by the circular streaking of spots shown in the [010] zone axis selected area electron diffraction (SAED) pattern (Figure 1 c). The exfoliated nanosheets exhibit the expected SAED pattern (Figure 1 d), suggesting that the MFI crystal structure is preserved, which was further confirmed by high-resolution transmission electron microscopy (HRTEM; Figure 1 e). AFM imaging showed that the exfoliated nanosheets have a uniform thickness of 3.2 nm (corresponding to 1.5 unit cells), which is in good agreement with earlier reports (data not shown here).[3,4,19] Bath sonication followed by horn sonication can cause further exfoliation of the piranha-solution-treated samples, whereas vortexing and shaking are not effective (Figure S6). These results demonstrate that the direct treatment of ML-MFI with piranha solution removed the majority of the OSDA from both inside and between the MFI nanosheets, leading to the formation of exfoliated MFI nanosheets with open pores. However, a fraction of non-exfoliated particles remained.

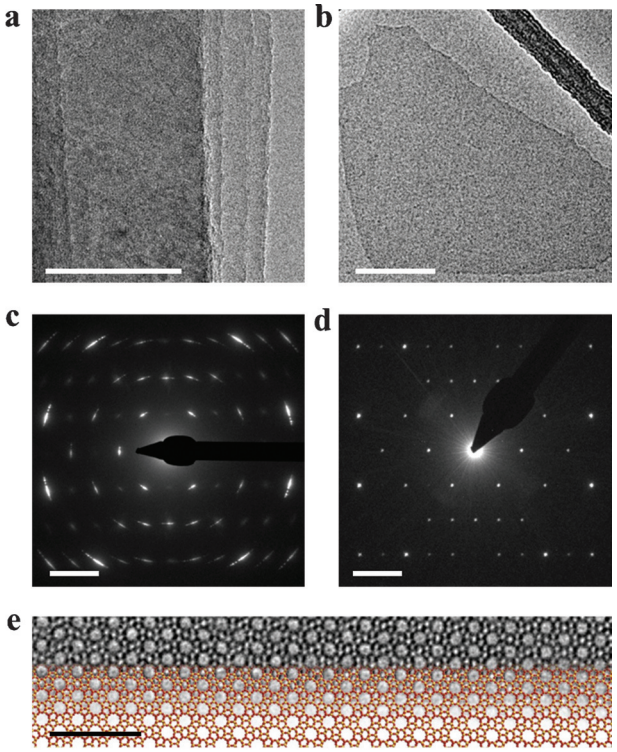

Figure 1. a, b) Conventional transmission electron microscopy (CTEM) images of non-exfoliated ML-MFI showing multiple sheets stacked together (a) and an exfoliated MFI nanosheet (b). Scale bars: 100 nm. c, d) [010] Zone axis diffraction patterns of non-exfoliated ML-MFI (c) and exfoliated nanosheets (d). Scale bars: 1 nm^{-1}. e) High-resolution Weiner filtered BF-TEM image of an exfoliated MFI nanosheet with the crystal structure superimposed viewed along the *b* axis of MFI. Scale bar: 5 nm.

A 3 μm coating on a porous polybenzimidazole (PBI) support was made by vacuum filtration of the aqueous suspension obtained after repeating the piranha solution treatment of ML-MFI four times (Figure S7). However, butane isomer single gas permeation tests showed no *n*-butane/isobutane selectivity. This could be attributed to defects formed by the remaining non-exfoliated particles (Figure S5 b). Future work on the purification of exfoliated nanosheets may overcome this problem, but here we decided to add a polymer melt-blending step before the piranha solution treatment (Figure 2 a), attempting to reduce the amount of remaining non-exfoliated particles. ML-MFI samples were mixed with oligomeric PS ($M_w \approx 1300\ g\,mol^{-1}$) inside a melt compounder, and the obtained nanocomposite was dissolved in toluene and washed by repeated centrifugation to remove the PS oligomer. The ethanol-washed cake of

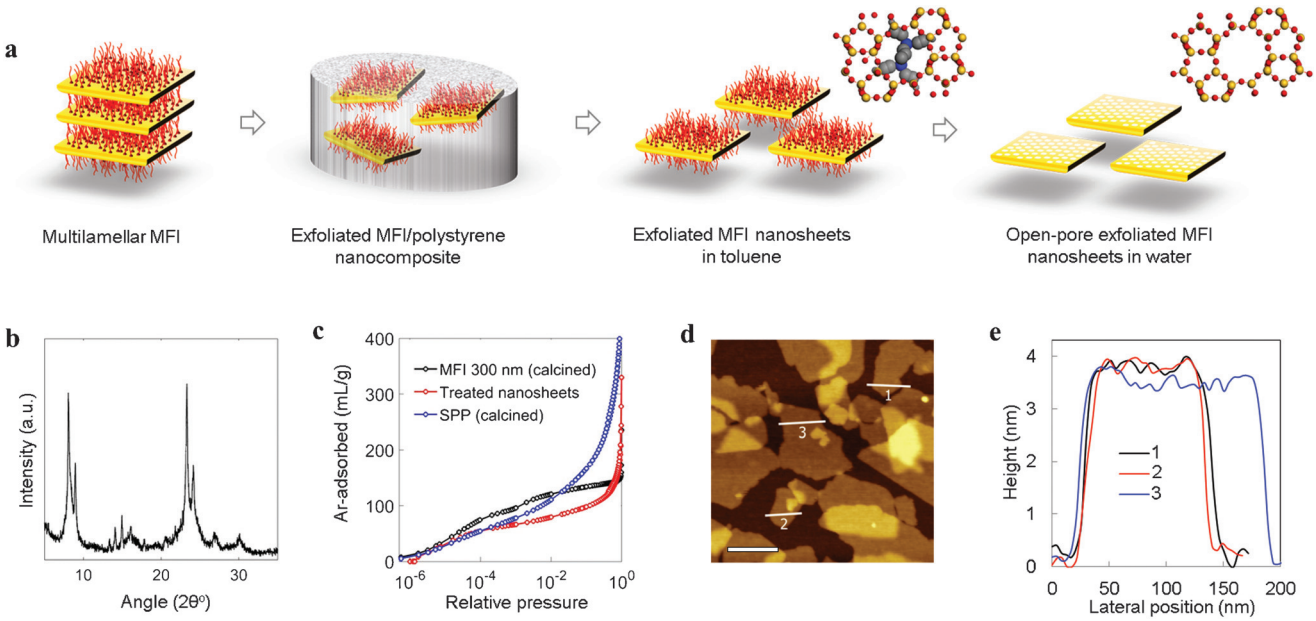

Figure 2. a) Preparation of an aqueous suspension of OSDA-free MFI nanosheets by treatment of exfoliated nanosheets with piranha solution. The ML-MFI is exfoliated by melt-blending with polystyrene (PS). After PS removal, a suspension of exfoliated MFI nanosheets in toluene is obtained. The exfoliated MFI nanosheets are further treated with piranha solution four times to remove the OSDA from the micropores. b) XRD pattern of the OSDA-free nanosheets after the treatment with piranha solution has been repeated four times. c) Argon adsorption isotherms of calcined 300 nm MFI particles, calcined self-pillared single-unit-cell MFI (SPP) particles, and exfoliated nanosheets that had been treated with piranha solution four times. d) AFM (tapping mode) topographical image of OSDA-free nanosheets (exfoliation followed by four treatments with piranha solution) coated on Si wafer by the use of a Langmuir trough. Scale bar: 200 nm. e) Plots of the height versus the length along the lines highlighted in (d).

the exfoliated nanosheets was further treated with piranha solution four times followed by washing and finally dispersed in deionized (DI) water (Figure S8). The resulting nanosheets preserved the MFI crystallinity as confirmed by their XRD pattern (Figure 2b). Their argon adsorption (80 mL g^{-1} adsorbed at $P/P_0 = 0.01$) is somewhat lower than that of typically calcined MFI and coincides with the adsorption isotherm of calcined 2D-MFI (SPP)[20] below $P/P_0 \approx 3 \times 10^{-4}$ (Figure 2c). The thickness of the resulting nanosheets is 3.2 nm as confirmed by AFM (Figure 2d), which is the typical 1.5 unit cell thickness of the single-layer nanosheets in ML-MFI. TEM imaging and electron diffraction (Figure S9) also confirmed the uniform thickness and MFI crystallinity after the treatment.

The OSDA-free nanosheet suspension can be used to form self-standing and supported films. For example, it was used to coat nanosheets onto porous silica support by vacuum filtration followed by drying at 80 °C for 3 h. A transparent film was formed that spontaneously peeled off from the silica support surface. This self-standing film (Figure 3a) is flat and crack-free. The cross-section SEM image (Figure 3b) shows that its thickness is about 5 μm and that it consists of closely packed oriented nanosheets.

The suspension can also be used to form films that do not peel off their supports. Figure 4 shows photographs and SEM images of a porous PBI support before and after nanosheet deposition. A uniform and well-packed nanosheet coating covers the PBI support (Figure 4b). It does not peel off and without any further treatment (i.e., without secondary growth or calcination), it exhibited a membrane separation performance that is characteristic of MFI micropores, with an *n*-butane over isobutane selectivity of 5.4 (Table S1). This ideal selectivity is about one order of magnitude smaller than that (ca. 47–62) achieved with well-intergrown MFI membranes obtained by secondary hydrothermal growth of a nanosheet deposit on ceramic supports followed by calcination.[21] However, it provides clear evidence that isomer-selective molecular sieving with a membrane consisting of 2D porous layers is feasible. The permeance of the current membrane is comparable to those of intergrown membranes. Further characterization is required to assess the reasons for the lower selectivity. Most likely, it is due to a combination of defects in between the layers providing non-selective transport pathways and partial blocking of selective pathways by overlapping nanosheets. Although gas separations using graphene oxide,[22,23] MOF exfoliated layers,[24] and calcined zeolite flake composite films[25] have been reported,

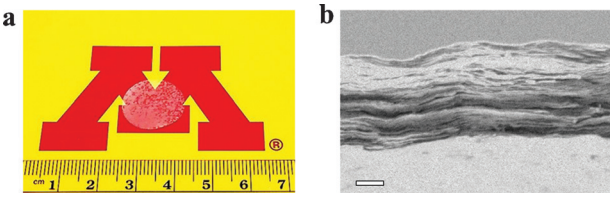

Figure 3. a) Photograph of a self-standing disc peeled off from a porous silica support after its formation by filtration. b) Cross-section SEM image showing the thickness of approximately 5 μm. Scale bar: 1 μm.

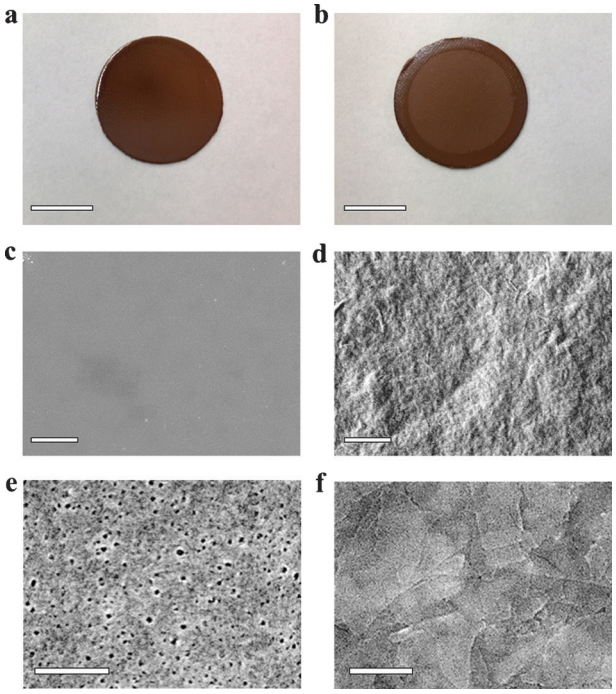

Figure 4. a, b) Photographs of the porous PBI support before (a) and after (b) filtration of an aqueous suspension of OSDA-free MFI nanosheets. Scale bars: 10 cm. c, d) Top-view SEM images of the porous PBI support before (c) and after (d) filtration of an aqueous suspension of OSDA-free MFI nanosheets. Scale bars: 2 μm. e, f) Magnified images of portions of (c) and (d), respectively. Scale bars: 200 nm.

selectivity for hydrocarbon isomers with directly deposited molecular sieves has not been demonstrated. As no secondary growth and high-temperature post-activation steps are required, such OSDA-free nanosheets should enable the large-scale fabrication of membranes on inexpensive polymer supports (flat sheets or hollow fibers), which could drastically reduce membrane manufacturing costs.[26] Further improvements in the nanosheet aspect ratio and packing are likely to result in an improved performance. Moreover, the water/nanosheet dispersions can be used in combination with other film formation approaches beyond the filtration coating method used here, including layer-by-layer, slip-coating, and Langmuir-trough-based methods to form MFI films for membranes and other applications. They can also be used in the formation of nanocomposites, including "selective flake" mixed matrix membranes.[25,27]

Acknowledgements

Support was provided by the ARPA-E program of the Department of Energy (DE-AR0000338 (0670-3240)) and, for certain membrane characterizations (porosimetry and SEM), by the Deanship of Scientific Research at the King Abdulaziz University (D-003/433). Q.X. and X.G. acknowledge support from the National Natural Science Foundation of China (NSFC, 21471131 and 21202116) and the China Scholarship Council. N.L. acknowledges support from the Jiangsu Overseas Research & Training Program for University Prominent Young & Middle-aged Teachers and Presidents and the NSFC (51573122). The TEM characterization (P.K.) was supported as part of the Catalysis Center for Energy Innovation, an Energy Frontier Research Center funded by the U.S. Department of Energy, Office of Science, Basic Energy Sciences (DE-SC0001004). Parts of this work were carried out in the University of Minnesota Characterization Facility, which receives partial support from the NSF through the MRSEC, ERC, MRI, and NNIN programs.

Keywords: membranes · nanosheets · separation · zeolites

How to cite: *Angew. Chem. Int. Ed.* **2016**, *55*, 7184–7187
Angew. Chem. **2016**, *128*, 7300–7303

[1] U. Díaz, A. Corma, *Dalton Trans.* **2014**, *43*, 10292–10316.
[2] M. Tsapatsis, *AIChE J.* **2014**, *60*, 2374–2381.
[3] K. Varoon et al., *Science* **2011**, *334*, 72–75.
[4] N. Rangnekar et al., *Angew. Chem. Int. Ed.* **2015**, *54*, 6571–6575; *Angew. Chem.* **2015**, *127*, 6671–6675.
[5] W. G. Kim, S. Nair, *Chem. Eng. Sci.* **2013**, *104*, 908–924.
[6] M. Choi, K. Na, J. Kim, Y. Sakamoto, O. Terasaki, R. Ryoo, *Nature* **2009**, *461*, 246–249.
[7] K. Na, W. Park, Y. Seo, R. Ryoo, *Chem. Mater.* **2011**, *23*, 1273–1279.
[8] R. J. Messinger, K. Na, Y. Seo, R. Ryoo, B. F. Chmelka, *Angew. Chem. Int. Ed.* **2015**, *54*, 927–931; *Angew. Chem.* **2015**, *127*, 941–945.
[9] K. Na, M. Choi, W. Park, Y. Sakamoto, O. Terasaki, R. Ryoo, *J. Am. Chem. Soc.* **2010**, *132*, 4169–4177.
[10] V. Nicolosi, M. Chhowalla, M. G. Kanatzidis, M. S. Strano, J. N. Coleman, *Science* **2013**, *340*, 1226419.
[11] J. T. Han et al., *Sci. Rep.* **2014**, *4*, 5133.
[12] J. N. Coleman et al., *Science* **2011**, *331*, 568–571.
[13] I. Ogino, Y. Yokoyama, S. R. Mukai, *Top. Catal.* **2015**, *58*, 522–528.
[14] R. Chalasani, A. Gupta, S. Vasudevan, *Sci. Rep.* **2013**, *3*, 3498.
[15] K. V. Agrawal, B. Topuz, Z. Jiang, K. Nguenkam, B. Elyassi, L. F. Francis, M. Tsapatsis, M. Navarro, *AIChE J.* **2013**, *59*, 3458–3467.
[16] S. Srivastava, N. A. Kotov, *Acc. Chem. Res.* **2008**, *41*, 1831–1841.
[17] M. A. Priolo, K. M. Holder, T. Guin, J. C. Grunlan, *Macromol. Rapid Commun.* **2015**, *36*, 866–879.
[18] A. Corma, U. Díaz, T. García, G. Sastre, A. Velty, *J. Am. Chem. Soc.* **2010**, *132*, 15011–15021.
[19] P. Kumar, K. V. Agrawal, M. Tsapatsis, K. A. Mkhoyan, *Nat. Commun.* **2015**, *6*, 7128.
[20] X. Zhang et al., *Science* **2012**, *336*, 1684–1687.
[21] K. V. Agrawal et al., *Adv. Mater.* **2015**, *27*, 3243–3249.
[22] H. W. Kim et al., *Science* **2013**, *342*, 91–95.
[23] H. Li, Z. Song, X. Zhang, Y. Huang, S. Li, Y. Mao, H. J. Ploehn, Y. Bao, M. Yu, *Science* **2013**, *342*, 95–98.
[24] Y. Peng, Y. Li, Y. Ban, H. Jin, W. Jiao, X. Liu, W. Yang, *Science* **2014**, *346*, 1356–1359.
[25] J. Choi, M. Tsapatsis, *J. Am. Chem. Soc.* **2010**, *132*, 448–449.
[26] A. J. Brown, N. A. Brunelli, K. Eum, F. Rashidi, J. R. Johnson, W. J. Koros, C. W. Jones, S. Nair, *Science* **2014**, *345*, 72–75.
[27] T. Rodenas, I. Luz, G. Prieto, B. Seoane, H. Miro, A. Corma, F. Kapteijn, F. X. Llabrés i Xamena, J. Gascon, *Nat. Mater.* **2015**, *14*, 48–55.

Received: February 1, 2016
Revised: March 6, 2016
Published online: April 21, 2016

